

Mechanisms of Electrical Breakdown in Low Vacuums

D. Ilić, D. Mostić, E. Dolićanin, K. Stanković, P. Osmokrović

Abstract: Justification of the hypothesis about the avalanche mechanism of vacuum breakdown is examined. For that purpose, values of dc and impulse breakdown voltage have been measured under well defined laboratory conditions, in the pressure range from 10^{-6} mbar to 1 bar, and for inter-electrode distances from 0.1 mm to 1 mm. Variable parameters of the experiment included the type of the residual gas and the material of the electrodes in the system used for forming a homogeneous electric field. Statistical analysis of experimental results and their comparison to the predictions of a theoretical model, attest that the avalanche mechanism of breakdown does come about in low vacuums.

Keywords: initial mechanisms, vacuum breakdown, vacuum avalanche mechanism, statistical analysis.

1 Introduction

Vacuum breakdown is initiated by the formation of a cloud of evaporated electrode material, within which breakdown develops through the avalanche mechanism of gas discharge [1,2,3]. The critical issued for this process is the creation of a sufficient starting amount of metal vapor, and for this purpose it is necessary to provide at least one of the electrodes with enough energy to cause its thermal instability. Thermal instability of one of the electrodes can be caused by the emission mechanism, by electrode material micro-particles accelerated in the electric field, or through the avalanche effect in the adsorbed residual gas layer on the electrodes [4,5,6].

The ground of all emission hypotheses is the notion that the electron emission current, caused by the electric field, produces thermal instability of one or both of the electrodes, followed by evaporation of electrode material into the inter-electrode region. Depending on the electrode at which thermal instability first occurs, an emission mechanism can be an initiatory breakdown mechanism of either cathode or anode type, corresponding to a cathode-type or an anode-type breakdown, respectively [7,8,9].

Manuscript received November 25, 2010; revised March 2, 2011; accepted April 7, 2011

D. Ilić is with the Metronik Inenjering, Belgrade, Serbia; E. Ć. Dolićanin is with the State University of Novi Pazar, Novi Pazar, Serbia; D. Mostić, K. Stanković, P. Osmokrović are with the Faculty of Electrical Engineering, University of Belgrade, Serbia;

During a cathode-type vacuum breakdown, thermal instability of the cathode occurs when the emission current from its micro-spikes exceeds a certain critical value at which they melt and evaporate due to the Joule effect [10,11,12,13]. The very initiation of vacuum breakdown is a consequence of cold electron emission from cathode micro-spikes, which is a quantum mechanical effect caused by the decrease of the potential barrier for electron emission, due to the presence of a high local electric field in the vicinity of micro-spikes with extremely small radii of curvature. Although the intensity of this cold emission current is not high, the small cross-section of micro-spikes accounts for high current density, which produces heating of micro-spikes and the emission of hot electron emission. Joule losses produce an irreversible temperature rise, amplifying the electron emission current and additionally increasing resistance of micro-spikes. This in turn causes further rise of Joule losses and leads to micro-explosions of micro-bulge peaks. The plasma that is thus formed is dense enough to enforce electric field at the electrode surface through the Debye field. The forming of cathode plasma ensues, which does not spread significantly from the cathode, while the cloud of anode plasma spans across the inter-electrode gap, finally producing the breakdown. Breakdown occurs virtually instantaneously after the critical value of emission current is reached, resulting in values of pulse, ac and dc breakdown voltages being practically equal. The time needed for micro-spikes' thermal instability to develop during the cathode initiated vacuum breakdown is short (0.1 - 100 μs), as is the time corresponding to the bridging of inter-electrode gap (20 - 500 μs). Hence, the initiation time for cathode vacuum breakdown is under 0.6 μs [14,15].

In the course of an anode-type breakdown, thermal instability of the anode is brought about by the cathode emission current, formed through the previously described mechanism, that causes local heating, melting and evaporation of an anode stain, while at the same time the emitting cathode micro-spikes are thermally stable. According to some authors, the processes at the anode depend upon the energy and current of the emitted electrons, which affect their penetration depth into the surface of the anode [16]. The evaporation at the anode precedes until sufficient density of anode material vapor appears so that the Townsend condition for gas breakdown is met. The time for a vacuum breakdown to initiate and develop through this mechanism is estimated at 10 μs [14,15,16].

There is always a multitude of loosely bound or free microparticles at the electrodes in vacuum, originating from the melting of material in previous breakdowns, switching operations, or the fabrication of the electrode system. When a voltage is fed to the electrodes, these microparticles are charged by electrostatic induction and then accelerated by the electrostatic force in the inter-electrode region. After gaining enough energy from the electric field, microparticles evaporate upon colliding with the electrodes. The change of electrode surface topography enhances emission mechanisms off the cathode, which additionally ionize the formed cloud of vapor. Plasma that is thus formed spreads until the Townsend condition for breakdown is fulfilled in it. The time for a vacuum breakdown to initiate through the micro-particle mechanism is estimated at 10 μs [17,18,19,20].

The hypothesis about the avalanche mechanism of vacuum breakdown rests upon the assumption that vacuum breakdown can be initiated by way of the avalanche effect in an

adsorbed gas layer or in impurities at the electrodes. This vacuum breakdown mechanism should be possible in systems that are not entirely pure or in low vacuums. The product of secondary electrode coefficients needs to be greater than 1, meaning that a charged particle drifting through the inter-electrode region produces multiplication upon collisions with molecules of adsorbed gas or impurities, giving rise to a larger amount of charged particles, eventually leading to breakdown. An estimated time for breakdown initiation and development through this mechanism would be about 1 μ s. The hypothesis about the avalanche mechanism of vacuum breakdown set up in this way has not been experimentally proven yet [21,22,23].

2 Experimental procedure and processing of measurement results

Investigations of the breakdown mechanism in constant vacuums included measurements of dc and impulse breakdown voltages, as well as of the emission characteristics V_{-4} , defined as the dc voltage value at which the emission current is 10^{-4} A, that in most cases is empirically shown to be approximately equal to one-half of the breakdown voltage. The emission characteristics V_{-4} is a stochastic quantity, since emission loci which define the emission current differ greatly in structure.

Investigations in the pressure range from 1 bar to 10^{-1} mbar were conducted in a specially constructed chamber with the possibilities of adjusting the inter-electrode gap and changing the electrodes. The chamber was designed for under-pressures, and was able to hold a constant pressure value of a work gas in the pressure range used in experiments for longer than 24 h, which was established empirically within 1 % type B relative measurement uncertainty (Fig. 1 a). The chamber was connected into a gas-vacuum circuit with built in mechanical and diffusion pumps that enabled the gas pressure in the chamber to be set with type B relative measurement uncertainty lower than 1 %.

For the 10^{-1} mbar to 10^{-6} mbar pressure range vacuum diodes with fixed electrode positions were used, produced specifically for the experiments with the desired pressures, residual gasses, electrode materials and inter-electrode gaps (Fig. 1 b). The glass enclosure (bulb) of the vacuum diodes was made of 8245 Jena Schott glass (laboratory molybdenum glass), while the metal leads were molybdenum wires (which ensured vacuum-tight sealing of the glass-metal junctions). Vacuum diodes were filled with working gasses and evacuated by the same procedure used for the previously described chamber. Gas evacuation was performed through a specially designed capilar that would be sealed off after baking at 480° C. Vacuum diode pressures were obtained with type B relative uncertainty lower than 1 %.

Residual gases in the chamber and vacuum diodes were the electronegative SF₆, electropositive N₂, and noble Ar. The electrode system, providing a homogeneous electric field, consisted of cylindrical electrodes made out of copper (with a 4.47 eV work function), elektron (1.8 eV work function), aluminium (3.74 eV work function), or tungsten (4.5 eV work function). Electrodes were polished to a high gleam prior to installation. During the experiment, the inter-electrode gap was varied from 0.1 mm to 1 mm, set with type

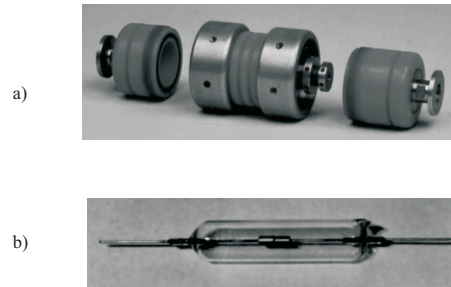


Fig. 1. a) Specially constructed chamber used for investigations in the pressure range from 1 bar to 10^{-1} mbar. b) Vacuum diodes used for investigations in the pressure range from 10^{-1} mbar to 10^{-6} mbar.

B relative measurement uncertainty below 0.1 %. Zero distance between the electrodes was determined by measuring ohmic resistance between them [24,25].

Dc voltage was obtained from a source with a maximum voltage of 30 kV and 3 kVA power. Dc voltage ripple was less than 1 %, and its rate of rise 8 kV/s. A two-stage Max type generator, constructed for the purposes of the experiment, was used as the impulse voltage source, adjusted at producing standard lightning impulse voltage (1.2/50 μ s). Dc and impulse voltage measurements were performed with combined relative uncertainty lower than 3 Experimental procedure consisted in the following:

1. Forming the electrode system within the chamber/vacuum diode (identical electrode systems were used in the chamber and in the diodes);
2. Connecting the chamber/vacuum diode to the gas-vacuum circuit;
3. Vacuuming the chamber/vacuum diode to 10^{-6} mbar in multiple steps and letting the working gas into it, to a pressure of 1 bar;
4. Setting the pressure of the residual gas in the chamber/vacuum diode;
5. In case of a vacuum diode, baking and sealing off the glass capilar;
6. Conditioning the electrode system with 100 consecutive breakdowns with an impulse voltage;
7. Measuring 1000 values of the dc breakdown voltage at 10^{-1} mbar pressure both in the chamber and in the vacuum diode, with other test parameters (inter-electrode gap, residual gas type, electrode material) equal for the chamber and the diode;
8. Measuring 1000 values of the dc breakdown voltage, with measurements of the emission characteristics V-4 after each tenth breakdown;
9. Repeating the previous measurement with reversed polarity of the dc voltage;
10. Measuring 1000 values of the impulse breakdown voltage, with measurements of the emission characteristics V-4 after each tenth breakdown;

11. Repeating the previous measurement with reversed polarity of the impulse voltage;
12. Setting the next working point (gas pressure and inter-electrode gap), and repeating the whole measurement procedure.

The procedure of processing the experimental results consisted in:

1. Applying the Chauvenet's criterion for discarding spurious measurement results from the statistical samples of random variables dc breakdown voltage, impulse breakdown voltage, and the emission characteristics [26,27];
2. Assessing by graphical and analytical methods if the sets of 1000 dc breakdown voltage values obtained at the pressure of 10^{-1} mbar for the electrode system in the chamber and the diode, with other test parameters equal, belong to a unique random variable. In case they don't, vacuum diodes produced for that series of measurements are discarded (and new ones are fabricated);
3. Dividing the 1000 values of random variables dc and impulse breakdown voltage into 20 statistical samples with 50 values each; dividing the 100 values of the random variable emission characteristics into 20 statistical samples with 5 values each; applying the U-test to examine whether the variables (or certain parts of variables, in case the U-test suggested an additive mixed distribution) belonged to a common statistical distribution;
4. Applying the chi-squared, Kolmogorov and the graphical test for examining the adherence of random variables, corresponding to the statistical samples, to the normal, Weibull, and double-exponential distribution [28];
5. Determining the parameters of statistical distributions identified for the random variables corresponding to the statistical samples, by using the momentum method and the maximum likelihood method [27,28];
6. Graphically representing the dependence of the parameters obtained for the statistical samples on the parameters of the experiment (pressure, inter-electrode gap, residual gas type, and electrode material).

3 Results and discussion

Fig. 2 shows the dependencies of dc and impulse breakdown voltage mean values on the pd product (the so called Paschen curves), along with the corresponding standard deviations, with the gas type as a variable parameter. Fig. 3 presents dc and impulse breakdown voltage mean values versus the pd product for various electrode materials. It is obvious from Figs. 2 and 3 that the range of pd product values considered in the experiment can be divided into three subregions, as far as the mechanism of breakdown is concerned. In subregion 1 the pd product can be described as a "good" variable, which means that the similarity law holds in

this region, i.e. that breakdown occurs through some of the gas mechanisms [29,30,31,32]. This is confirmed by the fact that the corresponding values of breakdown voltage for various

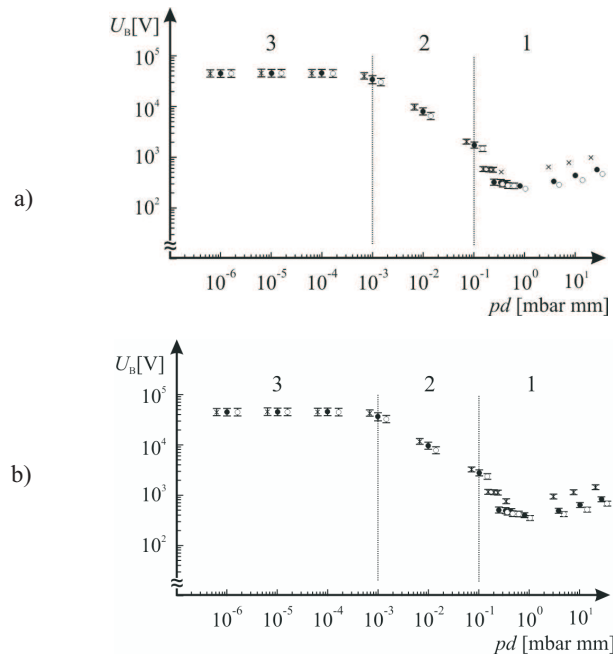


Fig. 2. a) Dependence of dc breakdown voltage mean value on the pd product (pressure \times inter-electrode gap), with the gas type as a parameter (o – Ar, • – N₂, x – SF₆), at the inter-electrode gap of 1 mm. b) Dependence of impulse breakdown voltage mean value on the pd product (pressure \times inter-electrode gap), with the gas type as a parameter (o – Ar, • – N₂, x – SF₆), at the inter-electrode gap of 1 mm.

gases differ in the way that would be expected according to their dielectric strengths. It can also be noted that in subregion 1 there is an influence of electrode material, depending on its work function, so that the material with the lowest work function also has lowest values of dc and impulse breakdown voltages, and vice versa, which again suggests that in this sub-region breakdown takes place via a gas mechanism, most probably Townsend type [33,34]. This is further substantiated by the fact that the impulse breakdown voltage behaves as a random variable in subregion 1, with values an order of magnitude larger than the corresponding values of dc breakdown voltage, which can be regarded a deterministic quantity. Such a difference between dc and impulse breakdown voltages is typical of the gas breakdown mechanism, and stems from the fact that the rise time of dc voltage is much longer than the time characteristic of the elementary gas discharge processes, so that the value of breakdown voltage doesn't depend on the stochasticity of free electron emergence and its transformation into an initiatory electron, as is the case with impulse voltages [35,36]. It is also evident that the change of voltage polarity doesn't affect the breakdown voltage value, as well as that the electrode system doesn't have to be conditioned again when the polarity is reversed. Stochasticity observed for some values of dc breakdown voltage arises because subregion 1 includes the Paschen minimum, to the left of which the so called anomalous

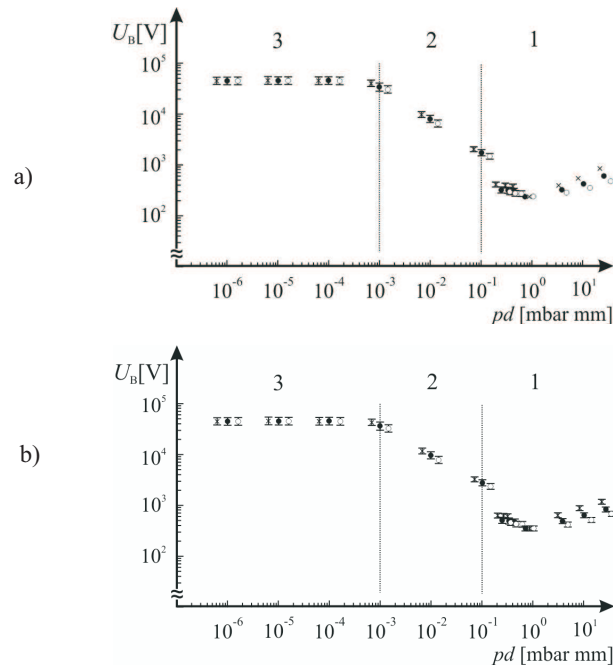


Fig. 3. a) Dependence of dc breakdown voltage mean value on the pd product, with the electrode material as a parameter (\circ - elektron, \bullet - aluminium, \times - tungsten), at the inter-electrode gap of 1 mm. b) Dependence of impulse breakdown voltage mean value on the pd product, with the electrode material as a parameter (\circ - elektron, \bullet - aluminium, \times - tungsten), at the inter-electrode gap of 1 mm.

Paschen effect occurs (the phenomenon of the spark taking a longer and energetically more favorable path of discharge) [37,38].

Subregion 2 is a kind of a transitional region. The pd product is no longer a "good" variable, but breakdown voltage still depends on the load voltage type, the type of the residual gas, and the material of the electrodes. Values of the breakdown voltage and the associated standard deviations are markedly larger than the corresponding values in subregion 1, i.e. much closer to the values expected in case of a vacuum mechanism of breakdown. However, the rate of breakdown voltage rise as a function of the inter-electrode gap (Fig. 4) is slower than would be expected for a vacuum mechanism. In subregion 2 the emission characteristics V-4 doesn't satisfy the 1/2 ratio with respect to the breakdown voltage, that is empirically established for vacuum emission mechanisms (Table 1). It has also been found that breakdowns in subregion 2 decondition the electrode system completely. This effect is more expressed at higher pressures (lower vacuums), while at lower pressures (better vacuums) the cathode is predominantly deconditioned.

In subregion 3 the pd product is no longer a "good" variable, and values of the breakdown voltage don't depend on load waveform, gas type, or electrode material. Furthermore, values of the breakdown voltage and the associated standard deviations are substantially larger than the corresponding values in subregions 1 and 2, and therefore comply with the values expected for a vacuum breakdown mechanism. The rate of breakdown voltage rise

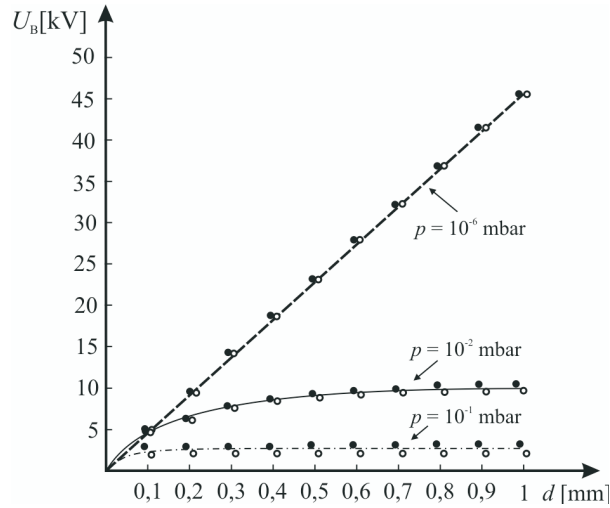


Fig. 4. Rate of breakdown voltage rise as a function of the inter-electrode gap (impulse (o) and dc (•) breakdown voltage mean values).

Table 1. Values of the dc breakdown voltage V_B and the emission characteristics V_{-4} at the inter-electrode gap of 1 mm for different values of residual gas pressure.

p [mbar]	10^{-6}	10^{-5}	10^{-4}	10^{-3}	10^{-2}	10^{-1}
V_B [kV]	45.6	45.4	45.7	38.9	9.8	2.1
V_{-4} [kV]	23.5	23.4	24.1	18.1	4.5	0.8

as a function of the inter-electrode gap agrees with the dependence expected for the cathode mechanism (Fig. 4). In subregion 3 the emission characteristics V_{-4} is again nearly equal to one-half of the corresponding breakdown voltage (Table 1). Moreover, complete deconditioning of cathode alone has been established in this subregion.

Fig. 5 shows the dependences of dc and impulse breakdown voltage mean values on the pressure of the residual gas (SF_6), along with the corresponding standard deviations, at constant inter-electrode gap. Fig. 6 shows the dependence of the dc breakdown voltage mean value on pressure, along with the corresponding standard deviations, with the type of residual gas as a parameter, while Fig. 7 presents that same dependence with the electrode material as a parameter. Results in these two figures demonstrate that in subregion 2 breakdown occurs through one of the vacuum mechanisms, or through a combination of these mechanisms, as well as that at higher pressures (lower vacuums) dependences of the breakdown voltage on experimental parameters resemble those for gas mechanisms of breakdown, while at lower pressures (higher vacuums) of subregion 3 this regularity vanishes and breakdown voltage becomes independent of experimental parameters. These results suggest that in subregion 2 breakdown may occur through a combination of the avalanche vacuum mechanism and the cathode vacuum mechanism. Avalanche vacuum mechanism dominates at higher pressures, and cathode mechanism at lower pressures. The aforementioned similarities in the dependencies of the breakdown voltage on experimental

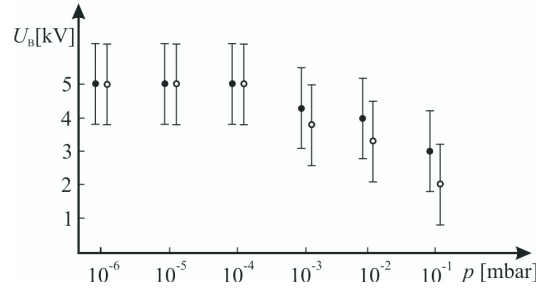


Fig. 5. Dependence of dc (\circ) and impulse (\bullet) breakdown voltage mean values and the corresponding standard deviations on pressure of the residual gas (SF_6), at the inter-electrode gap of 0.1 mm.

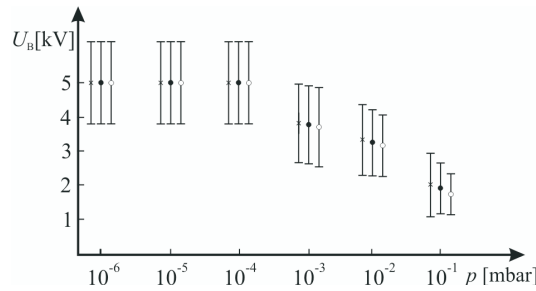


Fig. 6. Dependence of the dc breakdown voltage mean value on pressure, with the residual gas type as a parameter (\circ - Ar, \bullet - N2, \times - SF_6), at the inter-electrode gap of 0.1 mm.

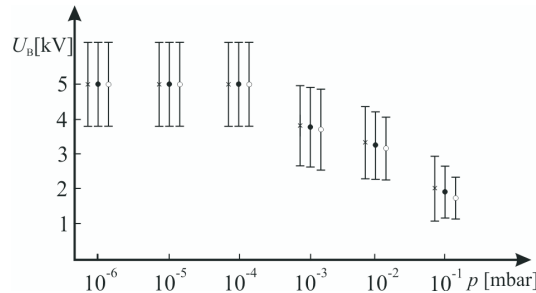


Fig. 7. Dependence of the dc breakdown voltage mean value on pressure, with the electrode material as a parameter (\circ - elektron, \bullet - aluminium, \times - tungsten), at the inter-electrode gap of 0.1 mm.

parameters at higher pressures to those for gas breakdown indicate that at these pressures breakdown predominantly occurs by way of the avalanche vacuum mechanism, while the deconditioning of the electrode system at the reversal of polarity signifies an additional presence of the cathode vacuum mechanism. Deconditioning of the electrode system at the reversal of voltage polarity suggests that only the cathode is conditioned during breakdown, since breakdowns eliminate the emission centers (microspikes) from it, while the anode remains practically intact [39]. This conclusion is corroborated by the form of dependence of the breakdown voltage on the inter-electrode gap shown in Fig. 4.

Fig. 8 presents the values of the χ^2 test variable (in relative units with relation to the

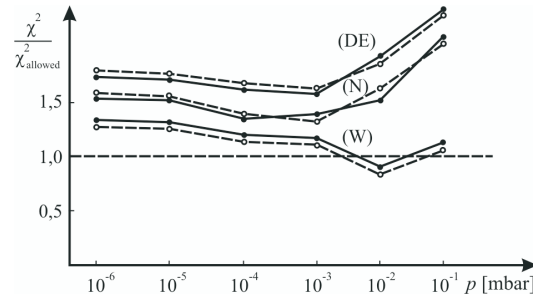


Fig. 8. Dependence of the χ^2 test variable (in relative units with relation to the maximum allowed value of the test variable, with a 5% level of significance) for random variables dc (---) and impulse (—) breakdown voltage on pressure, at the inter-electrode gap of 1 mm; (DE) double exponential distribution, (N) Normal distribution, (W) Weibull distribution.

maximum allowed value of the test variable, with a 5% level of significance) for random variables dc and impulse breakdown voltage in subregions 2 and 3. Data in this figure demonstrate that these random variables belong to the Weibull distribution at 10^{-4} mbar, adhere loosely to the Weibull distribution at 10^{-3} mbar, cease to belong to any distribution at 10^{-2} mbar, and belong to the Weibull distribution again at 10^{-1} mbar.

According to corresponding histograms, experimental results obtained for impulse breakdown voltage values at pressures 10^{-4} mbar, 10^{-2} mbar, and 10^{-1} mbar, for the inter-electrode gap of 0.1 mm, are presented on the Weibull probability plotting paper and shown in Fig. 9. Applied U-test (for statistical samples of impulse breakdown voltage values divided into 20 subsamples with 50 values each) with a 5% level of significance gave positive outcome at pressure values of 10^{-4} mbar and 10^{-1} mbar, while for 10^{-2} mbar pressure the outcome of U-test was negative. Fig. 9 shows that for 10^{-4} mbar pressure the impulse breakdown voltage random variable belongs to a unique Weibull-type distribution, which is also the case at 10^{-1} mbar, while at 10^{-2} mbar it belongs to an additive mixed distribution consisting of two Weibull-type distributions with slopes corresponding to the slopes of the mixed distribution at this pressure. Similar results arise from statistical analysis of the random variable emission characteristics V_{-4} are shown in Fig. 10.

Estimated parameters of the Weibull distribution, to which the dc breakdown voltage random variable belongs, are presented in Table 2 for different values of the inter-electrode gap, at pressures 10^{-4} mbar and 10^{-1} mbar. Parameter values in Table 2 don't differ from the corresponding values for the impulse breakdown voltage random variable.

Data in Table 2 show that the location parameter X_0 and the scale parameter η of the Weibull distribution depend approximately linearly on the inter-electrode gap at 10^{-4} mbar, while at 10^{-1} mbar such a dependence is not observed. The same data also suggests that if the macroscopic critical field was adopted as the random variable, instead of the breakdown voltage, it could have been described by a unique Weibull distribution for all series of measurements at 10^{-4} mbar, with the location, scale and shape parameters (E_0 , η_E and δ_E ,

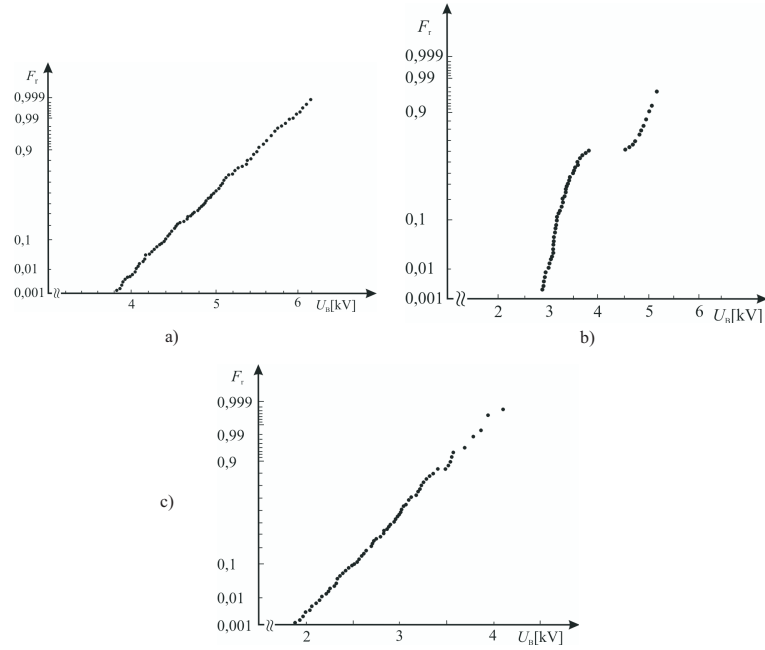


Fig. 9. Impulse breakdown voltage presented on the Weibull probability plotting paper at pressures: a) 10^{-4} mbar, b) 10^{-2} mbar, and c) 10^{-1} mbar, for the inter-electrode gap of 0.1 mm.

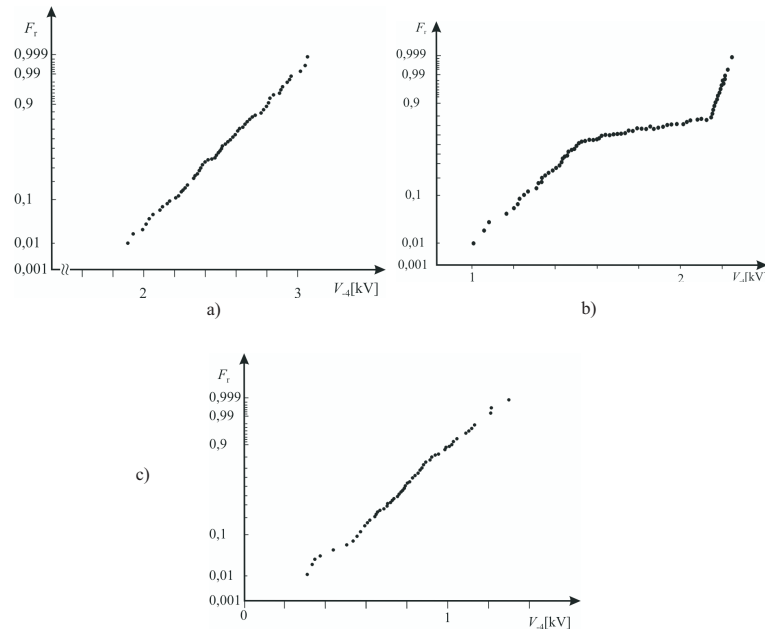


Fig. 10. Emission characteristics presented on the Weibull probability plotting paper at pressures a) 10^{-6} mbar, b) 10^{-2} mbar, and c) 10^{-1} mbar, for the inter-electrode gap of 0.1 mm.

Table 2. Estimated values of the Weibull distribution parameters for the dc breakdown voltage at 10^{-4} mbar and 10^{-1} mbar pressure.

pressure	10^{-4} mbar			10^{-1} mbar		
d [mm]	X_0 [kV]	η [kV]	δ	X_0 [kV]	η [kV]	δ
0.1	4.688	4.288	5.42	2.01	2.7	3.44
0.2	8.608	7.824	5.38	2.03	3.92	3.35
0.3	13.488	11.968	5.18	2.03	7.11	3.41
0.4	17.568	15.968	5.25	2.05	9.72	3.37
0.5	22.432	20.512	5.45	2.06	12.01	3.34
0.6	26.304	24.4	5.32	2.05	12.2	3.38
0.7	30.8	28.448	5.16	2.08	15.8	3.45
0.8	34.608	31.968	5.52	2.09	18.7	3.25
0.9	38.912	36.064	5.41	2.09	19.8	3.28
1.0	44	40.672	5.60	2.10	22.37	3.42

respectively) expressed as

$$E_0 = \frac{X_0}{d}, \quad \delta_E = \delta, \quad \eta_E = \frac{n}{d}$$

According to the weak spot theory this indicates that the macroscopic electric field is a quantity that characterizes weak insulation spots [40]. At 10^{-3} mbar, 10^{-2} mbar and 10^{-1} mbar pressures a dependence such as this has not been observed.

4 Conclusion

On the basis of the obtained results it can be concluded that in the investigated range of pressures and inter-electrode gaps breakdown occurs by way of the gas mechanism (sub-region 1) and the vacuum mechanism (subregions 2 and 3). In subregion 1 breakdown takes place through the Townsend mechanism, which is evident from the dependence of breakdown voltage in this subregion on the electrode material work function. The anomalous Paschen effect, another phenomenon that characterizes the Townsend mechanism of gas breakdown, also appears in subregion 1. Conditions are more complex in subregion 2, where a combination of two vacuum breakdown mechanisms occurs. At higher pressures (lower vacuums) breakdown occurs through the vacuum avalanche mechanism. This assertion is confirmed by the fact that for these pressures the pd product (pressure inter-electrode gap) is no longer a "good" variable, which means that electric discharge no longer takes place via a gas mechanism, since the similarity law, i.e. the Paschen law, no longer holds, and breakdown voltage becomes dependent on the inter-electrode gap alone, which is typical of vacuum mechanisms of breakdown. However, the observed effects of the load voltage type, insulating gas type, and electrode material on the breakdown voltage random variable indicate that, for the 10^{-1} mbar pressure, the gas adsorbed at the electrodes has a decisive role in breakdown initiation. These conclusions are corroborated by the statistical

analysis of the breakdown voltage random variable in this pressure range. The analysis shows that, for the 10^{-1} mbar pressure, breakdown occurs through a unique vacuum mechanism that is not cathode-type, since both electrodes are conditioned during breakdowns, while anode-type breakdown mechanism and microparticle mechanism are ruled out due to the ratio of the rate of the applied impulse voltages and the time constant of the anode mechanism, and the preparation of electrode surfaces (polishing to a high gleam), respectively. For the 10^{-4} mbar pressure, breakdown undoubtedly occurs through the cathode mechanism. This is confirmed by the following facts: statistical distribution of the breakdown voltage random variable is a unique Weibull distribution, i.e. all random variables belong to a single distribution; there is no significant difference between the random variables dc and impulse breakdown voltage; breakdown voltage random variables depend linearly on the inter-electrode gap, with a slope that is expected for a cathode breakdown mechanism; breakdowns are initiated at just one type of weak spots, and only the cathode is deconditioned by breakdowns. For pressures of 10^{-3} mbar and 10^{-2} mbar breakdown occurs through a combination of the cathode and the avalanche mechanism, which is evident from the adherence of the breakdown voltage random variables to additive mixed Weibull-type statistical distributions. Transition from the avalanche vacuum mechanism to the cathode mechanism in subregion 2 is most probably a consequence of a decrease of the adsorbed gas layer caused by the decrease in pressure.

Acknowledgment The Ministry of Science and Technological Development of the Republic of Serbia supported this work under contract 141046.

References

- [1] J.M Meek, J.D. Craggs, *Electrical Breakdown of Gases*, John Wiley & Sons, New York, 1978.
- [2] C.S Brown, *Introduction to Electrical Discharges in Gases*, Wiley, New York, 1965.
- [3] Little, R.P.; Whitney, W.T. J. App. Phys. 1963, 34, 2430-2434.
- [4] Jttner, B. *Vacuum arc initiation and applications* pp. 516-519 in Latham, R.V. High Voltage Vacuum Insulation: Basic Concepts and Technological Practice, Academic Press, London, 1995.
- [5] Djogo, G.; Cross, J.D., *Dependence of Gap Voltage Collapse During Vacuum Breakdown on Geometry and Plasma Dynamics*, IEEE Trans. Dielect. El. In. 1997, 4, 848-853.
- [6] Djogo, G.; Cross, J.D. *Circuit Modeling of a Vacuum Gap During Breakdown*, IEEE Trans. Plasma Sci. 1997, 25, 617-624.
- [7] Osmokrović P., *Influence of Switching Operations on the Vacuum Dielectric Strength*, IEEE Trans. on Power Delivery, 1993, 8, 175-181.
- [8] Osmokrović, P.; Vujisić, M.; Cvetić, J.; Pešić, M., *Stochastic nature of electrical breakdown in vacuum*, IEEE Trans. Dielect. El. In. 2007, 14, 803-812.
- [9] Osmokrović, P.; Djogo, G. *Vacuum* 1990, 40, 228.
- [10] Mesyatt, G.A. *Cathode Phenomena in a Vacuum Discharge: the Breakdown, the Spark and the Arc*, Nauka, Moscow, 2000.

- [11] Fursey, G.N., *Field emission and vacuum break-down*, IEEE Trans. Dielect. El. In. 1985 EI-20, 659-670.
- [12] Vujisić, M., Stanković, K., Vasić, A., *Comparison of gamma ray effects on eproms and eeproms*, Nucl. Technol. Radiat. Prot. 2009, 24, 61-67.
- [13] Vujisić, M., Stanković, K., Dolićanin, E., Jovanović, B., *Radiation Effects in Polycarbonate Capacitors*, Nucl. Technol. Radiat. Prot. 2009, 24, 209-211
- [14] Tsuruta, K. *Prebreakdown Field Emission Current and Breakdown Mechanism of a Small Vacuum Gap*, IEEE Trans. Dielect. El. In. 1983 18, 204-208.
- [15] Latham, R.V. HV, *Vacuum Insulation -The Physical Basis*, Academic Press, London, 1981.
- [16] Slade. P.G., *The Vacuum Interrupter: Theory, Design and Application*, CRC Press, 2008.
- [17] Olendzkaya, N.F., *Vacuum Breakdown with Transfer of Conducting Particles between Electrodes*, Radio Eng. & Electron. Phys. 1963, 8, 423.
- [18] Davies, D.K., Biondi, M.A., *Mechanism of DC electrical breakdown between extended electrodes in vacuum*, J. Appl. Phys. 1971, 42, 3089-3107.
- [19] Davies, D.K., Biondi, M.A., *Emission of Electrode Vapor Resonance Radiation at the Onset of DC Breakdown in Vacuum*, J. Appl. Phys. 1977, 48, 4229-4233.
- [20] Yen, Y.T., Tuma, D.T., Davies, D.K., *Emission of electrode vapor resonance radiation at the onset of impulsive breakdown in vacuum*, J. Appl. Phys. 1984, 55, 3301-3307.
- [21] Lafferty J.M. (Ed.). *Vacuum arcs - theory and application*, Wiley, New York, 1980.
- [22] Rozanova, N.B.; Granovski, V.L. *Sov. Phys. Tech. Phys.* 1956, 1, 471.
- [23] Bouchard, K.G., *Vacuum Breakdown Voltages of Dispersion-Strengthened Copper vs Oxygen-Free, High-Conductivity Copper*, J. Vac. Sci. Technol., 1970, 7, 358.
- [24] Stanković, K.; Vujisić, M.; Dolićanin, E. *Reliability of semiconductor and gas-filled diodes for over-voltage protection exposed to ionizing radiation*, Nucl. Technol. Radiat. Prot. 2009, 24, 132-137.
- [25] Stanković, K.; Vujisić, M., *Influence of radiation energy and angle of incidence on the uncertainty in measurements by GM counter*, Nucl. Technol. Radiat. Prot. 2008, 23, 41-42.
- [26] Rice, J.A. *Mathematical Statistics and Data Analysis*, Second Edition, Duxbury Press, Belmont, California, 1995.
- [27] Montgomery, D.C.; Runger, G.C. *Applied Statistics And Probability for Engineers*, John Wiley & Sons Inc, New York, 2006.
- [28] Ye, K., Myers, R.H., Walpole, R.E., Myers, S.L., *Probability & Statistics for Engineers & Scientists*, Prentice Hall, 2006.
- [29] Osmokrović, P., Krivokapić, I., Krstić, S., *Mechanism of Electrical Breakdown Left of the Paschen's Minimum*, IEEE Trans. Dielect. El. In. 1994, 1, 77-82.
- [30] Osmokrović, P., Ivić, T., Lončar, B., Vasić, A., *The validity of the similarity law for the electrical breakdown of SF6 gas*, Plasma Sources Sci. T. 2006, 15, 703-713.
- [31] Osmokrović, P., Arsić, N., Lazarević, Z., Kartalović, N., *Triggered Vacuum and Gas Spark Gaps*, IEEE Trans. on Power Delivery 1996, 11, 858-865.
- [32] Osmokrović, P., Kartalović, N., Atanackov, N., Ostojić, D., *Model Law for Gas Isolated Systems*, IEEE Trans. Plasma Sci. 2000, 28, 298-302.

- [33] Townsend, J.C., *Theory of Glow Discharge from Wires*, The Electrician, 1913, 348-350
- [34] Osmokrović, P., Vasić, A., Ivić, *The Influence of the Electric Field Shape on the Gas Breakdown under Low Pressure and Small Inter-Electrode Gap Conditions*, T. IEEE Trans. Plasma Sci. 2005, 33, 1677-1681.
- [35] Osmokrović, P., Vujisić, M., Stanković, K., Vasić, A., Lončar, B., *Mechanism of electrical breakdown of gases for pressure for 10 to 1 bar and inter-electrode gaps from 0,1 to 0,5 mm*, Plasma Sources Sci. T. 2007, 16, 643-655.
- [36] Osmokrović, P., *Electrical Breakdown of SF6 at Small Values of Product pd*, IEEE Trans. on Power Delivery 1989, 4, 2095 - 2100.
- [37] Osmokrović, P., Vasić, A., , IEEE Trans. Plasma Sci. 2005, 33, 1672-1676.
- [38] Osmokrović, P., *Mechanism of Electrical Breakdown of Gases at Very Low Pressure and Inter-electrode Gap Values*, IEEE Trans. Plasma Sci. 1993, 21, 645-654.
- [39] Farral, G.A., *Vacuum Arcs-Theory and Applications*, (J. M. Laferty ed.), Section "Electrode Conditioning", pp. 51-56, Wiley, New York, 1980.
- [40] Hauschild W., Mosch, W., *Statistical Techniques for High-Voltage Engineering*, IEE Power Series 13, Peter Peregrinus, London, 1992.